Catena 172 (2019) 87–96

Contents lists available at ScienceDirect

Catena

journal homepage: www.elsevier.com/locate/catena

Effect of riparian vegetation on stream bank stability in small agricultural catchments

Dominika Krzeminska[a,*], Tjibbe Kerkhof[b], Kamilla Skaalsveen[a], Jannes Stolte[a]

[a] Department of Soil and Land Use, Division of Environment and Natural Resources, Norwegian Institute of Bioeconomy Research, NO-1431 Aas, Norway
[b] Soil Physics and Land Management Group, Wageningen University, 6700 AA Wageningen, Netherlands

ARTICLE INFO

Keywords:
Stream bank stability
Agricultural catchments
Root reinforcement
Pore water pressure

ABSTRACT

The hydrological processes associated with vegetation and their effect on slope stability are complex and so difficult to quantify, especially because of their transient effects (e.g. changes throughout the vegetation life cycle). Additionally, there is very limited amount of field based research focusing on investigation of coupled hydrological and mechanical influence of vegetation on stream bank behavior, accounting for both seasonal time scale and different vegetation types, and none dedicated to marine clay soils (typically soil type for Norway).

In order to fill this gap we established hydrological and mechanical monitoring of selected test plots within a stream bank, covered with different types of vegetation, typical for Norwegian agricultural areas (grass, shrubs and trees). The soil moisture, groundwater level and stream water level were continuously monitored. Additionally, soil porosity and shear strength were measured regularly. Observed hydrological trends and differences between three plots (grass, tree and shrub) were analysed and formed the input base for stream bank stability modeling. We did not find particular differences between the grass and shrub plot but we did observe a significantly lower soil moisture content, lower soil porosity and higher shear strength within the tree plot. All three plots were stable during the monitoring period, however modeling scenarios made it possible to analyse potential differences in stream bank stability under different vegetation cover depending on root reinforcement and slope angle.

1. Introduction

Soil moisture content, pore water pressure and frictional properties of the soil are the most important factors influencing slope stability (e.g.: Simon et al., 1999; Bogaard and van Asch, 2002; Krzeminska, 2012). Slope stability is determined by the balance of shear stress and shear strength. Gravity, mobilised friction, buoyancy and seepage are the forces that work on soil body. The potential soil movement is resistant by the shear strength of the soil that can be mobilised along the slip surface. Negative pore water pressures reflect the surface tension of pore water in the voids, creating a suction effect on surrounding particles and contribute to the stability of the stream bank. Increase of the soil moisture content within the bank reduces the tension of pore water in the voids and decreases frictional soil strength. Additionally, presence of pore water increases the unit weight of the bank material making the bank more susceptible to failure.

Vegetation effects on slope stability may be broadly classified as either mechanical or hydrological (e.g.: Greenway, 1987; Gray and Sotir, 1996; Abernethy and Rutherfurd, 2000; Genet et al., 2008). The mechanical effect of vegetation on slope stability relates mainly to root reinforcement (positive influence; Thorne, 1990; Abernethy and Rutherfurd, 2000; Genet et al., 2008; Vergani et al., 2012).Roots anchor themselves into the soil to support above-ground biomass, producing a reinforced soil matrix that is less prone to shear failure (Waldron, 1977; Wu and Watson, 1998). The magnitude of root reinforcement mostly depends on root distribution, root mechanical properties (Greenway, 1987; Bischetti et al., 2005; Ji et al., 2012; Naghdi et al., 2013) and root moisture content (Pollen, 2007). Few studies (e.g. Pollen, 2007) talk about the weight of the vegetation mass having negative influence on slope stability. The hydrological effect of vegetation on slope stability relates to altering soil moisture. Presence of vegetation may reduce soil moisture content because of interception and transpiration, and water absorption by roots. On the other hand, riparian zones intent to favor infiltration over surface runoff: these may result in higher moisture contents during and after rainfall events and gives the potential for destabilization (Greenway, 1987; Collison and Anderson, 1996; Andreassian, 2004).

The quantification of coupled hydrological and mechanical effects

* Corresponding author.
E-mail address: dominika.krzeminska@nibio.no (D. Krzeminska).

https://doi.org/10.1016/j.catena.2018.08.014
Received 19 March 2018; Received in revised form 22 June 2018; Accepted 13 August 2018
Available online 21 August 2018

of vegetation on stream bank stability remains difficult due to the complexity of the interactions occurring between riparian vegetation and processes of bank stability (e.g.: Sidle, 1991; Abernethy and Rutherfurd, 2000; Sidle et al., 2006; Pollen, 2007). The beneficial and disadvantageous effects of vegetation presence act against each other (Simon and Collison, 2002) and can vary greatly in time: (1) pore water pressures are transient in response to changes in precipitation and streamflow and (2) root reinforcing depends on the vegetation growth cycle (Pollen-Bankhead and Simon, 2009). There is limited amount of field scale research focusing on coupled hydrological and mechanical influence of vegetation on stream bank stability, and even less dedicated to stream bank stability in small agricultural catchments, accounting for: (1) different vegetation types and (2) temporal changes in hydrological responses observed in both the bank and the stream.

In the framework of the forecasted increase in both the amount and intensity of precipitation events in Norway, all the natural phenomena triggered by water, including soil erosion, floods and landslide, are expected to boost their impact on the anthropic environment (e.g.: Øygarden et al., 2011; Hanssen-Bauer et al., 2015). The area along streams are among the landscape elements that first will be affected by climate change: stream bank failures often occur following floods (Tohari et al., 2007) or during prolonged rainfalls (Midgley et al., 2012). Vegetated buffer zones are one of the most common measures in Norway to improve water quality in agricultural catchments (e.g.: Blankenberg et al., 2016). While these measures aim to slow down the runoff and retain the sediment and nutrient particles from adjacent agricultural fields, they might have significant influence on stream bank stability, depending on the vegetation type.

The main cause of the streambank failures observed in small agricultural catchments in Eastern Norway is undercutting of bank toe and resulting steepening of the slope (Fig. 1; Skarbøvik et al., 2014; Skarbøvik, 2016) while the triggers are either hydrological factors (snow melt, intensive/prolonged rainfall) or human activity (using heavy machinery close to the edge of streambanks). Majority of the erosion events are observed in spring and autumn when the flooding risk is high (Skarbøvik and Bechmann, 2010): during the drawdown phase, the confining pressure of the water in the streams disappears and (partly-) saturated stream banks tent to fail (e.g. Jia et al., 2009). Relatively planar failure surface are commonly observed in the area (Fig. 1).

This paper aims to investigate both hydrological and mechanical effect of vegetation on stream bank stability in an agricultural catchment in Norway. We combine seasonal hydrological monitoring (soil moisture content and pore water pressure under three vegetation treatments, and water level in the stream) with stream bank stability modeling. Monitoring of groundwater level and soil moisture fluctuations accounts for infiltration of precipitation and/or runoff from agricultural field, and influence of changes in water level in the stream. A custom made version of the stream bank stability model (BSTEM) allows for incorporation of monitored hydrological responses.

2. Case study area and monitoring sites

Monitored test plots are located along the Hobøl River, the main tributary of the Morsa catchment system, located in South-Eastern Norway. The catchment area of the Hobøl River is 333 km^2. About 16% of the catchment is agricultural land, about 5% waterbodies, and the remaining 79% forest (Blankenberg et al., 2008). The dominating soil type within the catchment is coarse moraine in the forested areas and marine deposits with silt loam and silty clay loam texture in agriculture areas (Hauken and Kværnø, 2013). Fluvial deposits with silt and silt loam texture are found along the river. The mean annual temperature is 5.6 °C, measured at Rygge meteorological station. The mean annual precipitation is 829 mm (Skarbøvik and Bechmann, 2010). Large differences in water discharge are observed at the Hobøl River (Skarbøvik et al., 2014): from relatively stable discharge (1.0–3.0 m^3/s) in winter and summer periods, to dynamically changing high discharge (7.0–48.0 m^3/s) in spring and autumn.

Hydrological monitoring of two plots representing vegetation typical for Norwegian agriculture areas (Fig. 2): mixed grass (root depth up to 20 cm) and trees (root depth more than 100 cm) were installed. Additionally, on the site with mixed grass, redcurrant berry bushes (*Ribes rubrum* '*Jonkheer van Tets*') have been planted (in July 2016). All plots are located within distance of 50 m to ensure similar soil and environmental conditions. The height of the bank, at all three test plots, is 4 m above riverbed, while the slope varies greatly: 27.5°–32.6° for the grass plot, 39°–54° for the trees plot and 24.7°–39.7° for the shrubs plot. No visible soil stratification was observed within vertical profiles during installation of the equipment.

3. Material and methods

3.1. Monitoring

Hydrological monitoring. Each test plot was installed with two piezometers (Fig. 3): one located close to the river (the bottom of these piezometers reached the average level of the water in the river during the dry summer period, 1.60 m above riverbed) and one located close to the top of the stream bank (the bottom of these piezometers was at c.a.2.30 m above riverbed). The piezometers were made of PVC tubes with 0.90 m filters, covered with standard filter protection, surrounded by filter sand and closed with granular bentonite. Groundwater responses were monitored with the use of automatic recording water pressure devices (Diver; Eijkelkamp, Netherlands) with a 10 min time resolution. Atmospheric pressure was monitored with Baro-DIVER (Eijkelkamp, Netherlands). Each test plot was equipped with soil moisture and soil temperature sensors (FDR, 5TM from Decagon Devices) in combination with EM50 Digital data Logger recording with 30 min time resolution. Based on generic calibration of the FDR the accuracy for the volumetric water measurements is ± 0.03m^3/m^3 while for temperature readings it is ± 1 °C. In order to monitor changes in soil moisture profiles within stream banks, sensors are installed at 5 depths

Fig. 1. Examples of observed undercutting processes and associated slope failures in small agricultural catchments in Eastern Norway: (a, b) Hobøl River and (c) Lier River.

Fig. 2. Location of the monitoring plots (a) and pictures from the plots: (b) grass plot, (c) trees plot, (d) shrubs plot.

(0.1, 0.2, 0.3, 0.4, 0.5 m in grass and bushes plots, and 0.3, 0.4, 0.5, 0.6 and 0.8 m in trees plot). Fluctuations of water level in the river were monitored with the use of Ultasonic Distance Sensor (UDL, from PIL Sensoren Gmbh, with accuracy of ± 2 mm). Time resolution for the water level was 30 min. As trade-off between sensor's measuring range (2.0 m) and installation possibilities the initial setup was able to monitor water level fluctuation in the stream above the 50.3 m a.s.l. From 11/03/2017 onwards, we increased the height of the sensor with 0.7 m due to damage by floating ice and risk of flooding the sensor. Additionally, we performed several manual measurements of water level in the stream during summer 2016.

Monitoring of mechanical properties of roots reinforced soil and bank erosion. In addition to monitoring related to hydrological properties, we performed regular investigations of in-situ undrained shear strength of the root-reinforced soil with a Field Inspection Vane Tester (FIVT, Eijkelkamp, Netherlands) and soil porosity measurements (bulk density rings, 100 cm^3). Additionally, we monitored potential changes in the bank profile with series of erosion pins, 6 pins per each plot (e.g.: Lawler, 1993; Skarbøvik, 2016) using a Topcon differential GPS system (from Topcon Positioning Systems).

Weather data. The meteorological parameters were monitored in-situ using a combination of Davis Rain Gauge Smart Sensor (0.2 mm resolution) and HOBO® Micro Station Data logger (ONSET Computer Corporation).

3.2. Stream bank stability modeling

3.2.1. BSTEM model

Stream bank stability modeling has received great attention since 1960 (Papanicolaou et al., 2006). Slope stability analysis, typically performed using the limit equilibrium method (LEM), aims to compute factor of safety as a ration between stabilising and destabilising forces. Improving their models, researchers tend to account for (1) better, more realistic, geometry including the presence of tension cracks (2) the effects of positive and negative pore water pressure and (3) presence of riparian vegetation. In this study, we used the bank stability sub-model of BSTEM (Bank-Stability and Toe-Erosion Model; Simon et al., 1999). BSTEM is a physically based single site model, that combines three limit equilibrium-methods to estimate the stability of the bank (factor of safety, F_S): horizontal layers (Simon et al., 2000), vertical slices (Langendoen and Simon, 2008) and cantilever shear failure (Thorne and Tovey, 1981). It is capable to model shear-type failures that occur when the driving force (stress) exceeds the resisting force (strength), assuming the planar failure surface.

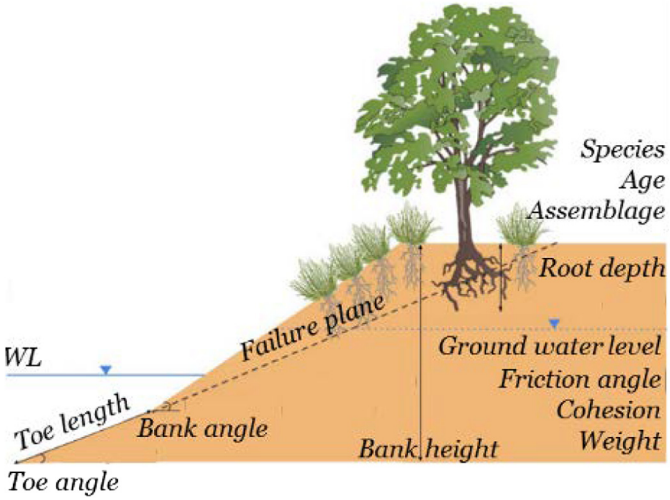

Fig. 4. A schematic bank diagram with the various inputs used in BSTEM. (Adapted from Lammers, 2015.)

BSTEM allows for five unique layers, accounted for pore water pressures on both the saturated and unsaturated parts of the failure plane, and the confining pressure from stream flow (Fig. 4). Driving forces in a stream bank are controlled by the total volume and the weight of soil in a failure block (determined by the height, angle, unit weight and mass of pore-water). The resisting strength of the bank material is determined using a modified Mohr-Coulomb criterion (Eq. (1)) for saturated conditions and Fredlund et al. (1978) criterion (Eq. (2)) for unsaturated conditions.

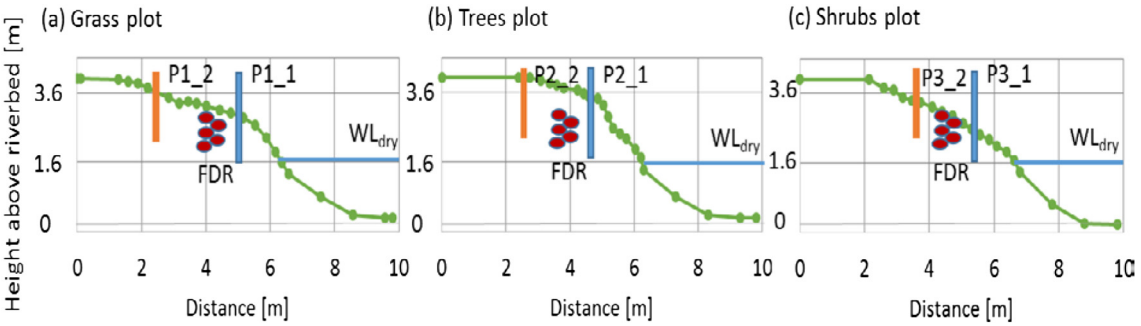

Fig. 3. The stream bank profiles with location of monitoring equipment for: (a) the grass plot, (b) the trees plot and (c) the shrubs plot. P stand for piezometers, WL_{dry}, refers to average water level in the river during the dry summer of 2016. Depth of FDR sensors is not scaled.

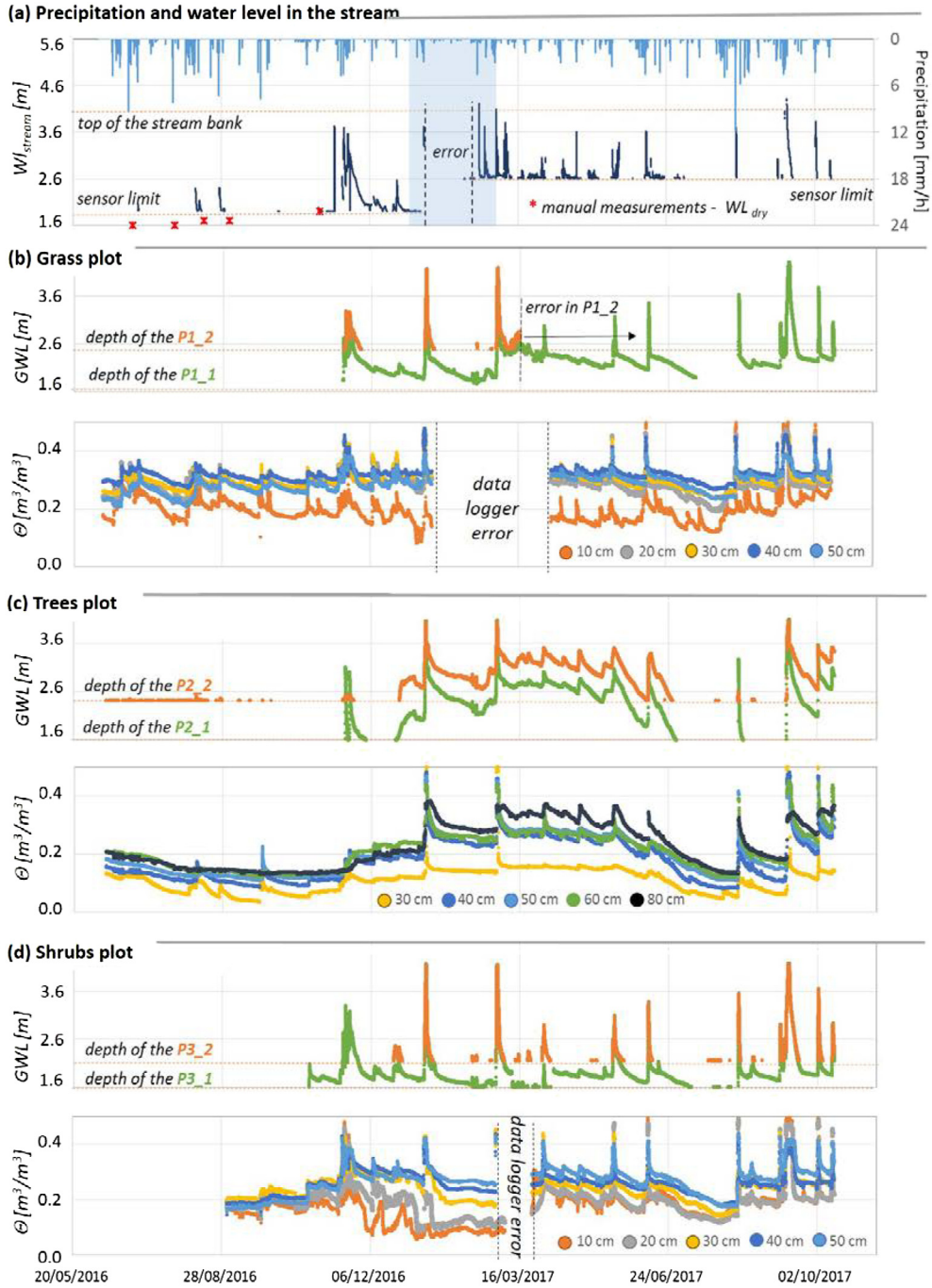

Fig. 5. Hydrological monitoring results: precipitation and fluctuation of water level in the Hobøl river (WL_{stream}) above the riverbed (a), blue shaded area indicates freezing period; fluctuation of groundwater level (GWL) above the riverbed and soil water content (Θ) at four depths within the grass plot (b), the trees plot (c) and the shrubs plot (d). (For interpretation of the references to colour in this figure legend, the reader is referred to the web version of this article.)

$$S_r = c' + (\sigma - \mu_w)\cdot\tan\varphi' \quad (1)$$

where: S_r is the shear strength of the soil [kPa], c' is effective cohesion [kPa], σ is normal stress [kPa], μ_w is pore-water pressure [kPa], and ϕ' is the effective friction angle [°].

$$S_r = c' + (\sigma - \mu_a)\cdot\tan\varphi' + (\mu_a - \mu_w)\cdot\tan\varphi^B \quad (2)$$

where: μ_a is pore-air pressure [kPa], $(\sigma - \mu_a)$ is the net normal stress on the failure plane, ϕ^b describes the rate of increase of shear strength from matric suction [°].

BSTEM assumes that water table is horizontal within a particular bank. The pore pressures are calculated for each layer based on provided depth of groundwater table, assuming hydrostatic conditions. BSTREM does calculate the water exchange between the stream and the bank. However, the custom made version of BSTEM allows for use of both the stream hydrograph and pore water pressure data series as an input parameter to the model and makes it possible to account for the pore water pressure fluctuation in the stream bank.

The model has built-in algorithm that iterates over multiple failure scenarios (shear emergence elevations and the angle of shear surface) to determine the one with the lowest F_S. The bank is considered to be '*stable*' if calculated *Fs* is greater than 1.3. Banks with *Fs* value between 1.0 and 1.3 are considered to be '*conditionally stable*', i.e. stable but with little safety margin for uncertain or variable data. Slopes with *Fs* value less than 1.0 are '*unstable*' (Simon et al., 2000).

The mechanical influence of vegetation on bank stability is included in BSTEM by changing the value of the soil strength parameters to account for root reinforcement using RipRoot model (Pollen and Simon, 2005). RipRoot is a fiber bundle model which predicts progressive root breakage and subsequent distribution of the applied load. Additional cohesion due to roots, c_r, is calculated based on plant age and percent contribution to assemblage.

However, within the current version of BSTEM, the root reinforcement is only designed and tested for top of bank vegetation, not vegetation covering an entire bank slope. In our case, vegetation cover stretched over the entire bank slope and reached the water when it was at its lowest stage. Therefore, we estimated total cohesion of root-reinforced soil (c_T) outside of the BSTEM, based on the following formula (Waldron, 1977; Schmidt et al., 2001; Hubble et al., 2010; Chok et al., 2015):

$$c_T = c' + c_r \quad (3)$$

where: c' is effective soil cohesion and c_r is additional root cohesion based on RipRoot model. We calculate c_T for each soil layer defined with BSTEM model and used it directly as an input to BSTEM bank material data tables.

3.2.2. Modeling strategy

As a first step we applied the custom made version of the bank stability sub-model of BSTEM for three existing plots to test the current stability of the banks. For further investigation and comparability analysis we have defined the following modeling scenarios:

- *shrubs future* – where we assumed fully developed root system of shrubs (see Table 3);
- *slope 24.7°* - where we performed slope stability analysis assuming the minimum (24.7°) slope angle for three existing plots and for *shrubs - future* scenario
- *slope 54.0°* - where we performed slope stability analysis assuming the maximum (54.0°) slope angle for three existing plots and for *shrubs - future* scenario

4. Results

4.1. Monitoring results

Fig. 5(a) shows series of precipitation and changes in water level in the river (WL_{stream}). WL_{stream} at the beginning of the observation period, summer 2016, is below or at the border of the sensor limit. In this period we collected a series of manual measurements (red asterisks on Fig. 4a), confirming that the water level in the stream was below the sensor limit and was in a range of 1.40–1.70 m above riverbed (WL_{dry}). Hydrological responses observed within the three plots (Fig. 5b, c, d) show both differences and similarities. The grass plot and shrubs plot show similar dynamics both in groundwater level (*GWL*) and soil water content (Θ) fluctuation, while clear differences in hydrological responses within the trees plot are observed. The timing of observed *GWL* peaks, in response to precipitations, is the same in all three test plots. However, *GWL* within the trees plot stayed at a higher level for a longer period than at the two other plots.

The observed trends of Θ variations correspond to the *GWL* fluctuations. There were visible differences in the Θ trends within 0–30 cm subsoil: significantly lower Θ at 0–10 cm depth within the grass plot, at 0–20 cm depth within the shrubs plot and at 30–40 cm depth within the trees plot (Table 1). These differences correlate with observed different root depths and, intuitively could be further explained by root water uptake influence. The period of relatively stable low Θ observed within the shrubs plot (Fig. 4c) in winter 2017 corresponded to the observed freezing period.

Fig. 6a shows the soil porosity values measured at two depths within each plot. In general, soil porosity decreased with increasing soil depth.

Table 1
Normalized soil moisture values, averaged over observation period.

	Normalized soil water content						
Depth	10 cm	20 cm	30 cm	40 cm	50 cm	60 cm	80 cm
Grass plot	0.26	0.41	0.45	0.49	0.44	–	–
Trees plot	–	–	0.16	0.28	0.33	0.35	0.39
Shrubs plot	0.22	0.25	0.36	0.39	0.33	–	–

Soil porosity at the trees plot was lower than at the other two plots. The results of vane shear strength measurements are shown at Fig. 5b. In all plots vane shear strength increased with soil depth. This behavior is a combined effect of soil compaction with depth (Table 2) and presence of the root-reinforced soil (different root depths for different vegetation cover type). The vane shear test measurements in the trees plot were the highest and showed the most variability, as they strongly depend on the position relative to main root systems. Fig. 6c shows the soil-roots strength changes with time. A clear trend is visible in all three plots: higher values of vane shear strength can be observed during late spring and summer. Again this trend is a combination of two factors: intensity of the vegetation grow (higher root density) and lower soil moisture content (Fig. 5).

Table 2 presents the characteristics of the soil within the three plots and included both measured (saturated unit weight, γ_{sat}) and estimated (c', ϕ') parameters. The ϕ' values are based on geotechnical data (Geotechdata, 2013)The c' values are based both on geotechnical data (Geotechdata, 2013) and field observations, taking the vane shear strength measured under (near-) saturation conditions and below the root depths as a rough approximation of the soil cohesion. Table 3 presents the root cohesion (c_r) as a result of species composition within each plot, calculated with the RipRoot sub-module of BSTEM.

The erosion pins showed no changes in the stream bank profiles for the monitoring period, which is in agreement with what we observed during the field visits.

4.2. Modeling results

4.2.1. Processing of the hydrological data and scenario description

In order to prepare the hydrological input series for the BSTEM model we had to fill the gaps in the monitoring data. The gaps correspond with the dry periods when the stream level dropped below the sensor measuring limit after re-installation of the ultrasonic sensor. In these periods, we filled the gaps with equal value of 1.6 m above riverbed, which is an average of the manual water level measurements during the dry summer period (Fig. 3). In this way, we created a worst case scenario: low water level in the stream means removal of the confining pressure from the stream. In addition, if there is no water observed in the piezometers (*GWL* is below the piezometer depth) we assume that *GWL* is equal piezometer depth.

4.2.2. Simulated stream bank stability

Fig. 7(a, b, c) presents F_S simulated for the three plots using the slope angles observed within each plot. Additionally, Fig. 7d presents predicted slope stability within the shrub area assuming full root development of freshly planted berry bushes (*shrubs - future* scenario). In all cases F_S is above 1.3 which means that all three plots are stable. This is in agreement with field observation and erosion pin measurement (Table 3). The variation in *Fs* values corresponds to the variation in observed *GWL* and WL_{stream} (Fig. 5). With an increase in observed WL_{stream} followed by an increase of *GWL*, the slope stability increases as confining pressure from the stream provides the support for the bank. When WL_{stream} decreases the level of stability depends on the timing of decrease in *GWL*. In case of the grass plot and the trees plot a general trend of lower *Fs* values during spring (from March to April 2017) and early autumn (September–November) and higher *Fs* values during the

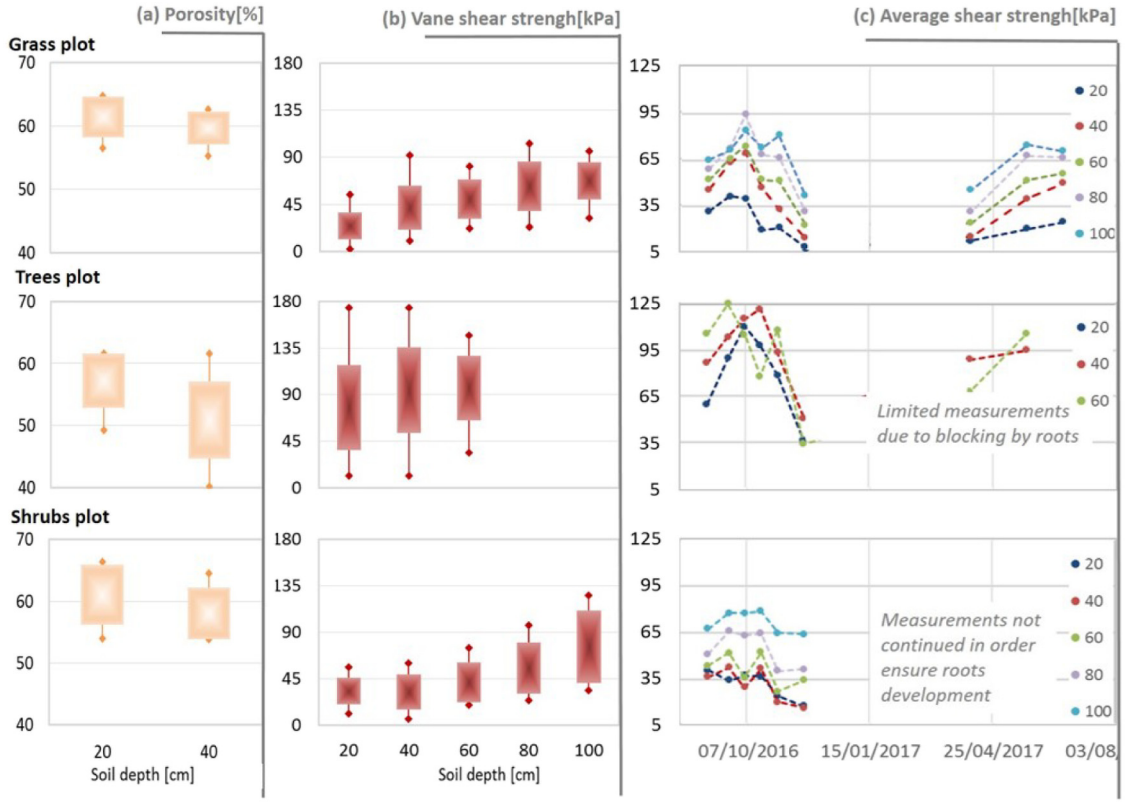

Fig. 6. Measured porosity (a) and vane shear strength (b) at different depths within three plots. Graphs show boxes of average values ± standard deviation, together with max and min measured values; (c) changes in average shear strength with time and with depth, for the three plots.

Table 2
Characteristics of the soil within the three plots and BSTEM input parameters.

Layer	Depth	Saturated unit weight			Friction angle (ϕ')			Cohesion (c')		
		Grass plot	Trees plot	Shrubs plot	Min[b]	Max[b]	BSTEM intput[(e)]	min[(m)]	min[(m)]	BSTEM intput[(e)]
	[m]	[kN/m^3]			[degrees]			[kPa]		
1	0.2	16.0[(m,av)]	16.6[(m,av)]	16.1[(m,av)]	18.0	32.0	26.4	2.0[(m)]	8.0[(m)]	4.3[(e)] [c]
2	0.4	16.0[(m,av)]	16.6[(m,av)]	16.1[(m,av)]	18.0	32.0	26.4	2.0[(m)]	8.0[(m)]	4.3[(e)] [c]
3	0.6	16.3[(m,av)]	17.8[(m,av)]	16.7[(m,av)]	18.0	32.0	26.4	2.0[(m)]	8.0[(m)]	4.3[(e)] [c]
4	1.6	18.0[(e)] [a]	18.0[(e)] [a]	18.0[(e)] [a]	18.0	32.0	26.4	–	–	4.3[(e)] [c]
5	4.1	18.0[(e)] [a]	18.0[(e)] [a]	18.0[(e)] [a]	18.0	32.0	26.4	–	–	4.3[(e)] [c]

[(m)]measured; [(av)]average value; [(e)]expert estimates.
[a] Schaap et al. (2001).
[b] Geotechdata (2013).
[c] Default BSTEM parameters.

Table 3
Additional cohesion from roots, based on RipRoots sub-model (Pollen-Bankhead and Simon, 2009).

	Vegetation cover			Addition root cohesion (c_r)
	Type	Age	%cover	[kPa]
Grass plot	Mixed grass	2 years	90	0.35
Trees plot	Alder/brich	25 years	40/40	7.18
Shrubs plot	Grass/berry bushes	2 years/ 1 year	40/60	0.35
Shrubs future	Grass/berry bushes	2 years/ 7 year	40/60	1.37

summer (May–June 2017) is observed. This trend is not as strong within the shrubs plot (Fig. 7c, d). There is an increase in simulated F_S values between current status of the shrub plot (Fig. 7c) and its potential behavior in case of a fully developed roots system of the berry bushes (Fig. 7d).

Fig. 8 presents the F_S values for the three plots calculated for the minimum and maximum slope angle observed across all three plots: 24.7° - measured within the shrub plot; and 54.0° - measured within the tree plot. Fig. 9 summaries all calculations (all plots and all scenarios) in form of histograms. Note that even with the longest periods of higher *GWL* (Fig. 5c) the tree plot shows the highest values of F_S for all simulated scenarios. When the steeper slope is considered for the grass plot and shrub plot, they start to show periods with *Fs* values in range between 1.0 and 1.3, indicating '*conditional stability*' of the slope and with *Fs* below 1.0, suggesting potential slope failure.

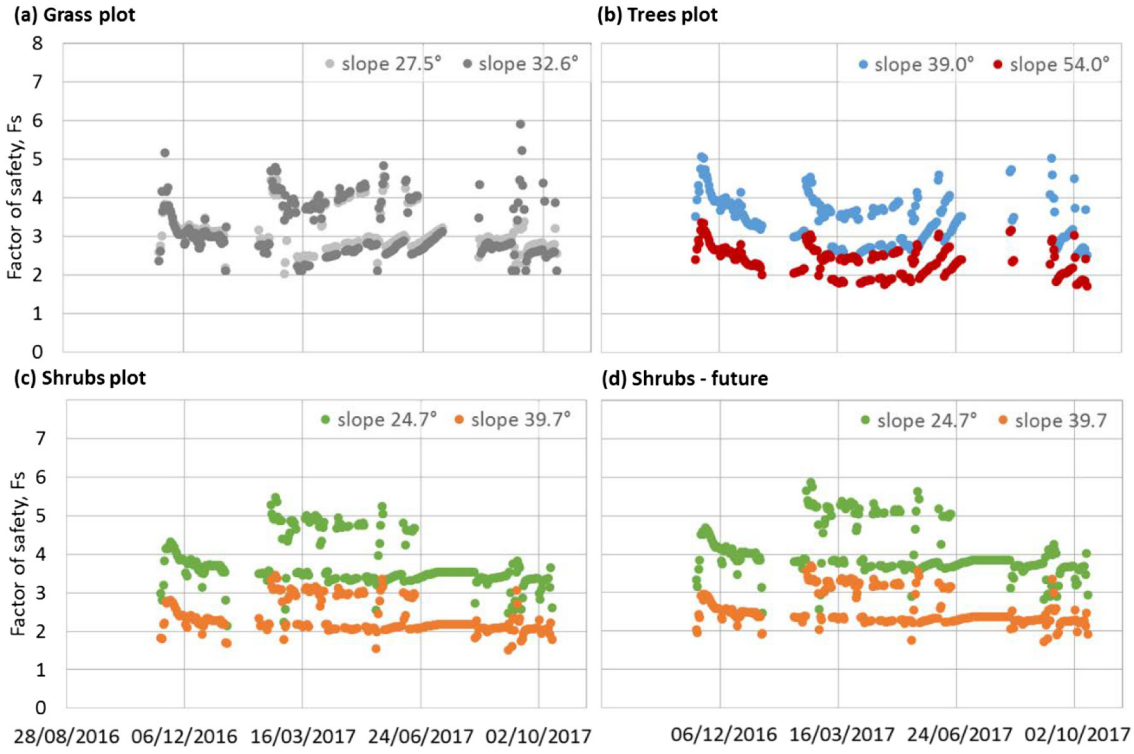

Fig. 7. Variation of *Fs* with time for the three existing plots (a, b, c) and for the "shrubs-future" scenario (d). Different colours emphasise different slope angles. (For interpretation of the references to colour in this figure legend, the reader is referred to the web version of this article.)

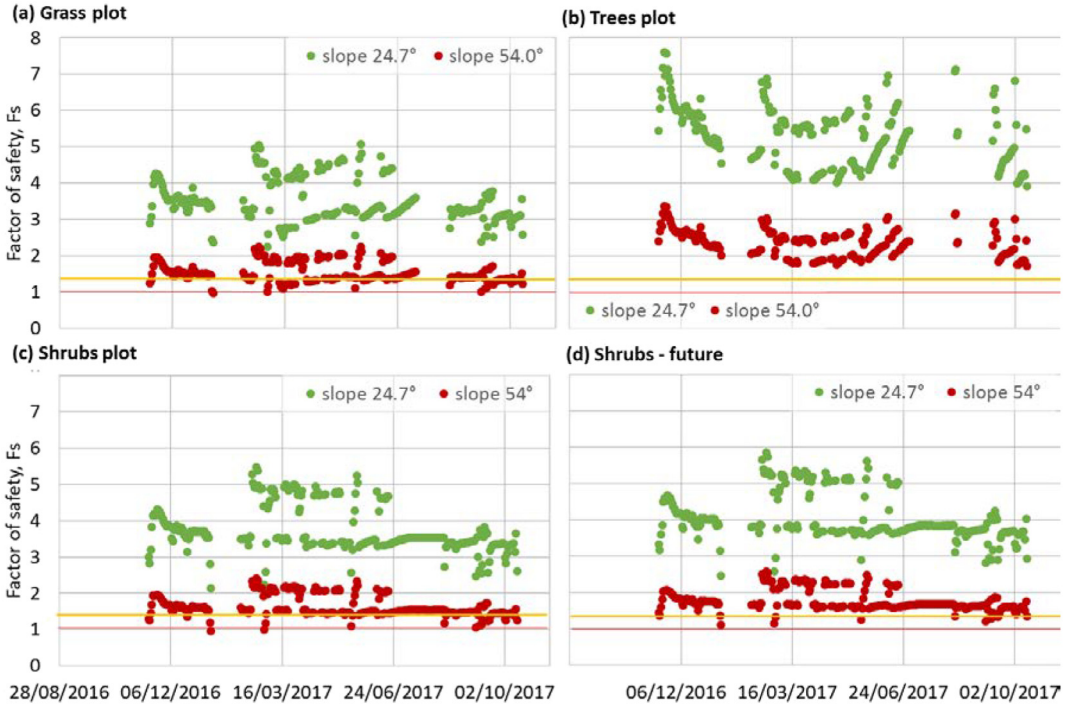

Fig. 8. Variation of *Fs* with time for modeling scenarios: slope 24.7° and slope 54.0° for three existing plots (a, b, c) and shrubs - future scenario (d). The threshold lines are indicated to the graphs: red - $F_S = 1$, 'unstable slope' and yellow - $F_S = 1.3$, 'conditionally stable slope'. (For interpretation of the references to colour in this figure legend, the reader is referred to the web version of this article.)

5. Discussion

We based our research on comparative analysis in order to see which type of vegetation is optimal for preventing stream bank failures, triggered by flooding or prolonged rainfall. Although we tried to select uniform test areas, differences between the plots were unavoidable. The most important difference is the slope of the bank, which is generally steeper in the trees plot than in the two other plots. This already indicates that trees covered buffer zones provide stronger reinforcement to the bank slopes than other vegetation. In order to overcome the

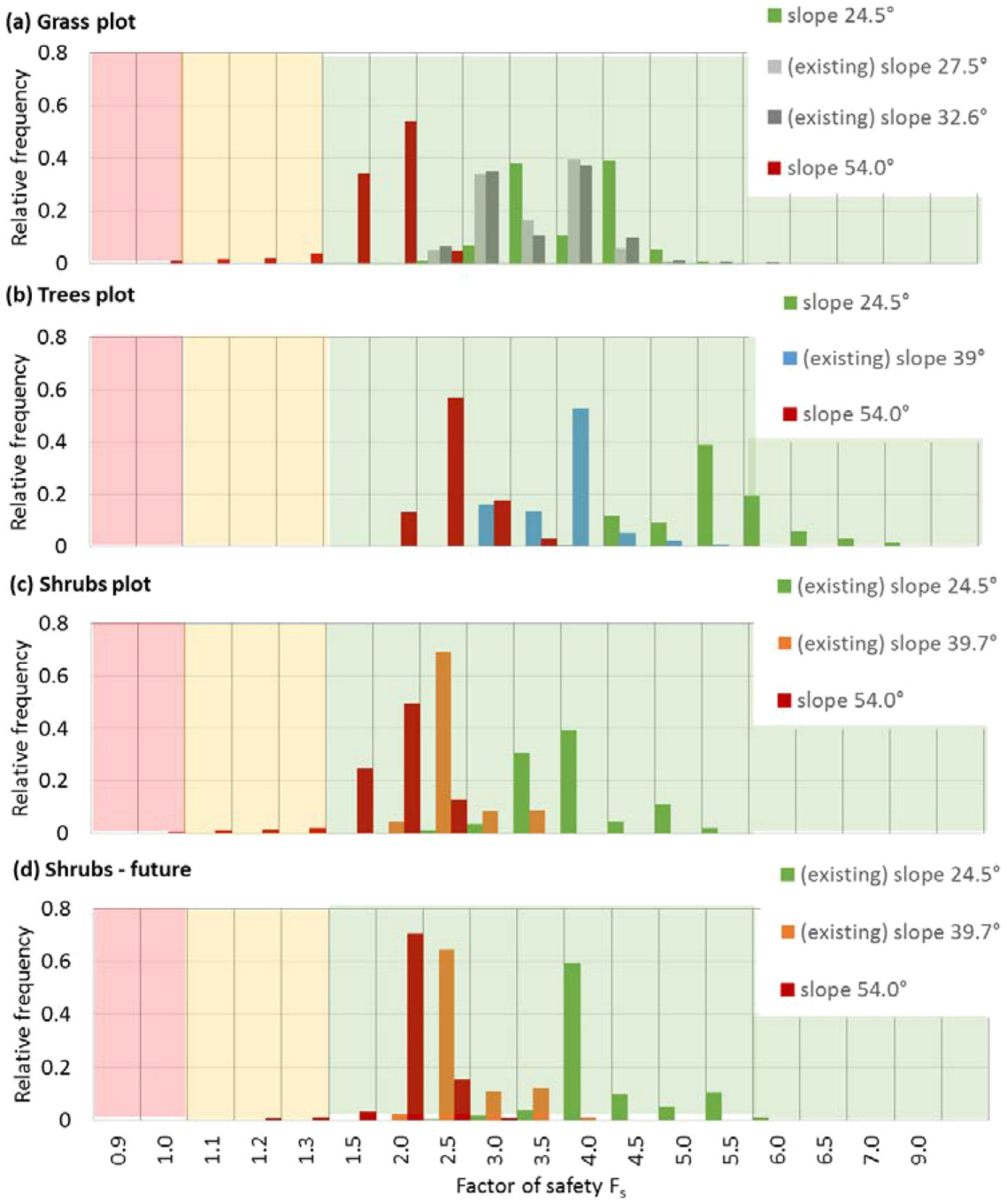

Fig. 9. Histograms of FS for all simulated scenarios. Shadowed areas indicate stability classes according to the BSTEM model: red – unstable slope; yellow – conditional stability; green – stable slope. (For interpretation of the references to colour in this figure legend, the reader is referred to the web version of this article.)

differences in slope angle we introduced different model scenarios (Fig. 8) and simulated potential variation in *Fs* in these slopes validated by the observed hydrological responses. However, changes in slope angle can result in a different distribution of pore water pressure and consequently differences in slope stability calculations.

Another difference between the selected plots appears when looking at the monitored variation in groundwater levels (Fig. 4b, c, d). While the grass and shrubs plot seem to represent similar hydrological systems, the trees plot behaves differently. The groundwater level in the trees plot is generally higher that in the two other plots. This is in contradiction with other findings of Simon and Collison (2002) who reported significantly lower matric potential within the tree cover area compared to grass cover area or bare soil control site of their experimental field. The reason for this discrepancy might be the size of vegetated zone along the river: we are looking at vegetated slopes of the stream banks only, not big forested areas. The size of vegetation strips defines the degree of its effect on local hydrology. Additionally, part of our observations can also be explained by a more compacted soil under the trees cover (Fig. 5a). Nevertheless, it is likely that we did not identify all the components of hydrological system in this area, i.e. subsurface groundwater recharge. This limits the possibility to compare hydrological effects between the plots.

As there was no stream bank covered with shrubs in the area, we have planted berry bushes at the beginning of the monitoring period. Not yet fully developed root systems of the planted berry bushes resulted in little to no differences in both hydrological responses (Fig. 4b,

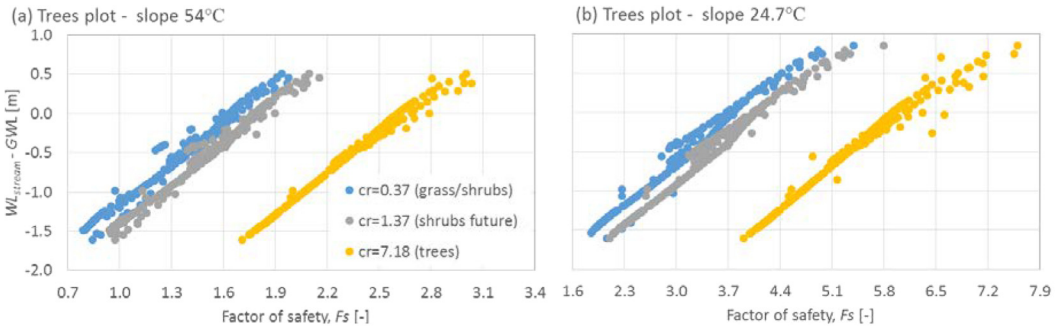

Fig. 10. Monitored differences between GWL and WL_{stream} vs. calculated F_S, depending on the level of additional root reinforcement, for slope angle of 54° (a) and 24.7° (b).

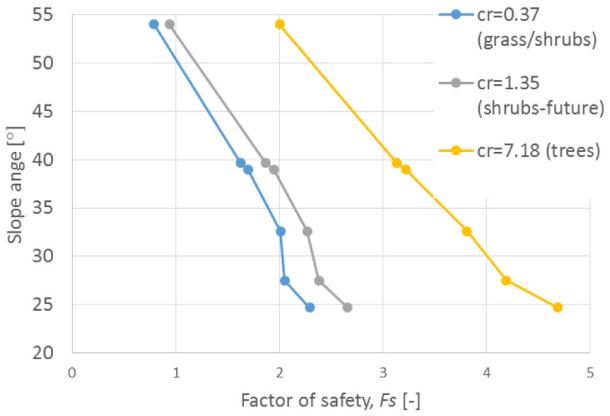

Fig. 11. Relationship between calculated F_S and potential slope angle, depending on the level of additional root reinforcement.

d), additional root cohesion (Fig. 5b, c and Table 3) and calculated safety factor values (Fig. 6a, c) between shrub and grass plot. Therefore, we added the '*shrubs - future*' scenario for the shrubs plot to account for a potential increase in strength of the root-reinforced soil with time (Table 3). However, we ignored the possible effect of fully developed root system on slope hydrology.

There are few limitations of the current version of BSTEM that influence the stability analysis. Presented modeling results do not account for potential seasonal changes in additional root cohesion, that we observe in the field (Fig. 6) and that is confirmed by other studies (e.g.: Pollen-Bankhead and Simon, 2009). During winter and early spring the vegetation is dormant and additional cohesion coming from the roots can be smaller or even negligible, especially in case of grass cover. Moreover, additional load coming from vegetation weight is not included in stability calculations. This, in turn, might be important in case of trees cover (e.g.: Ott, 2000; Pollen, 2007). It is also necessary to mentioned pre - assumed planar failure plan as a general limitation of BSTEM model. However, in in our case, this assumption is valid as planar plane are commonly observed in the area (Fig. 1).

The observed hydrological responses together with slope stability analysis suggest that investigated vegetated buffer zones give mostly a mechanical aid to bank stabilization, with the hydrologic effects considered as less important. Slope stability depends on the differences between *GWL* and WL_{stream} and hydrological effects should be visible in lowering of *GWL*. In our case, the trees plot showed the most stable stream bank conditions (Fig. 8), even with the higher groundwater levels, as a result of simulated high root reinforcement (Table 4). Every 0.8 kPa of additional root cohesion (difference between $c_{r,grass} = 0.37$ kPa and $c_{r,shrubs\text{-}future} = 1.35$ kPa) can compensate between 20 cm (in case of slopes with 54.0° inclination) and 25 cm (in case of slopes with 24.7°) of *GWL* increase (Fig. 10). Moreover, Additional cohesion from the roots compensates the slope inclination and the level of the compensation differ depending on the reference slope angle (Fig. 11).

6. Conclusion

The coupled hydrological and mechanical effect of vegetation on bank stability is complex and varies greatly in time depending on soil characteristics, hydrological conditions and vegetation type. With this study we aimed to investigate stream bank stability under different vegetation cover types (grass, trees and shrubs) and its time variation depending on the hydrological conditions and vegetation stage.

Based on field data analysis and stream bank stability modeling we conclude that vegetation covering the slopes of the stream banks has mostly a mechanical effect on stream bank stability. Among monitored plots, representing stream banks covered with grass, trees and shrubs, the area with the trees is the most stable and shows the highest capacity to accommodate potential shear stress. This indicates that the type of the vegetation, corresponding to level of root reinforcements that should be used for reinforcing the stream bank slope depends on slope angle: for gentle angles the grass cover is sufficient treatment, while trees cover is necessary to protect steeper slopes against slope failures.

This research indicates the need for further studies to improve knowledge about the soil-roots reinforcement, and its variability in time, taking into account the range of typical Norwegian soils and most common Norwegian plant species. A combination of field and laboratory test (i.e. triaxial test, root strength measurements, etc.) is necessary for better quantification of the mechanical effect of roots for stream bank stabilization in Norway.

Acknowledgements

The research leading to these results has received funding from the European Union Seventh Framework Programme (FP7/2007–2013) under grant agreement no. 603498 (RECARE project). The authors also thank Dr. Eddy J. Langendoen from United States Department of Agriculture (USDA) with preparing custom made version of BSTEM.

References

Abernethy, B., Rutherfurd, I.D., 2000. The effect of riparian tree roots on the mass-stability of riverbanks. Earth Surf. Process. Landf. 25, 921–937.
Andreassian, V., 2004. Waters and forest: from historical controversy to scientific debate. J. Hydrol. 291, 1–27.
Bischetti, G.B., Chiaradia, E.A., Simonato, T., Speziali, B., Vitali, B., Vullo, P., Zocco, A., 2005. Root strength and root area ratio of forest species in Lombardy (Northern Italy). Plant Soil 278, 11–22.
Blankenberg, A.-G., Turtumøygard, S., Pengerud, A., Borch, H., Skarbøvik, E., Øygarden, L., Bechmann, M., Syversen, N., Vagstad, N.H., 2008. Tiltaksanalyse for Morsa: Effekter av fosforreduserende tiltak i Morsa 2000–2006 (Mitigation analysis for the Morsa Catchment: Effects of measures to reduce phosphorus levels in the period 2000–2006; in Norwegian). Bioforsk Rapp. 86 (3) (54 pp.).
Blankenberg, A.-G., Paruch, A., Paruch, L., Deelstra, J., Haarstad, K., 2016. Nutrients tracking and removal in constructed wetlands treating catchment runoff in Norway.

In: Vymazal, J. (Ed.), Natural and Constructed Wetlands. 978-3-319-38926-4, .
Bogaard, T.A., van Asch, T.W.J., 2002. The role of the soil moisture balance in the unsaturated zone on movement and stability of the Beline landslide, France. Earth Surf. Process. Landf. 27, 1177–1188. https://doi.org/10.1002/esp.419.
Chok, Y.H., Jaksa, M.B., Kaggwa, W.S., Griffiths, D.V., 2015. Assessing the influence of root reinforcement on slope stability by finite elements. Int. J. Geo-Eng. 6, 12. https://doi.org/10.1186/s40703-015-0012-5.
Collison, A.J.C., Anderson, M.G., 1996. Using a combined slope hydrology and stability model to identify suitable conditions for landslide prevention by vegetation cover in the humid tropics. Earth Surf. Process. Landf. 21, 737–747.
Fredlund, D.G., Morgenstern, N.R., Widger, R.A., 1978. The shear strength of unsaturated soils. Can. Geotech. J. 15, 313–321.
Genet, M., Kokutse, N., Stokes, A., Fourcaud, T., Cai, X., Ji, J., Mickovski, S., 2008. Root reinforcement in plantations of *Cryptomeria japonica* D. Don: effect of tree age and stand structure on slope stability. For. Ecol. Manag. 256, 1517–1526.
Geotechdata, 2013. Angle of friction. http://geotechdata.info/parameter/angle-of-friction.html, Accessed date: 7 June 2013.
Gray, D.H., Sotir, R.B., 1996. Biotechnical and Soil Bioengineering Slope Stabilization: A Practical Guide for Erosion Control. John Wiley & Sons, Toronto, pp. 365.
Greenway, D.R., 1987. Vegetation and slope stability. In: Anderson, M.F., Richards, K.S. (Eds.), Slope Stability. John Wiley & Sons, New York, pp. 240.
Hanssen-Bauer, I., Førland, E.J., Haddeland, I., Hisdal, H., Mayer, S., Nesje, A., Nilsen, J.E.Ø., Sandven, S., Sandø, A.B., Sorteberg, A., Ådlandsvik, B., 2015. Klima i Norge 2100. NCCS Report No. 2/2015.
Hauken, M., Kværnø, S., 2013. Chapter 2: Agricultural management in the JOVA catchments. In: Bechmann, M., Deelstra, J. (Eds.), Agriculture and Environment. Long Term Monitoring in Norway. Akademika Publishing, Trondheim, 978-82-321-0014-9, pp. 19–42.
Hubble, T.C.T., Docker, B.B., Rutherfurd, I.D., 2010. The role of riparian trees in maintaining riverbank stability: a review of Australian experience and practice. Ecol. Eng. 36, 292–304.
Ji, J., Kokutse, N., Genet, M., Fourcaud, T., Zhang, Z., 2012. Effect of spatial variation of tree root characteristics on slope stability. A case study on Black Locust (*Robinia pseudoacacia*) and Arborvitae (*Platycladus orientalis*) stands on the Loess Plateau, China. Catena 92, 139–154.
Jia, G.W., Zhan, L.T., Chen, Y.M., Fredlund, D.G., 2009. Performance of a large-scale slope model subjected to rising and lowering water levels. Eng. Geol. 106, 92–103.
Krzeminska, D.M., 2012. The Influence of Fissures on Landslide Hydrology. Delft University of Technology, Netherlands (PhD Thesis).
Lammers, W., 2015. Uncertainty and Sensitivity in the Bank Stability Model: Implications for Estimating Phosphorus Loading. Colorado State University, Fort Collins, Colorado (MSc thesis).
Langendoen, E.J., Simon, A., 2008. Modeling the evolution of incised streams. II: Streambank erosion. J. Hydraul. Eng. 134 (7), 905–915.
Lawler, D.M., 1993. The measurement of river bank erosion and lateral channel change: a review. Earth Surf. Process. Landf. 18, 777–821.
Midgley, T.L., Fox, G.A., Heeren, D.M., 2012. Evaluation of the bank stability and toe erosion model (BSTEM) for predicting lateral retreat on composite streambanks. Geomorphology 145–146, 107–114. https://doi.org/10.1016/j.geomorph.2011.12.044.
Naghdi, R., Maliki, S., Abdi, E., Mousa, R., Nikkoy, M., 2013. Assessing the effect of Alnus roots on hillslope stability in order to use in soil bioengineering. J. For. Sci. 59, 417–423.
Ott, R.A., 2000. Factors affecting stream bank and river bank stability, with an emphasis on vegetation influences. In: Welbourn, Freeman M. (Ed.), Region III Forest Resources & Practices Riparian Management Annotated Bibliography, pp. 21–40 (Online version, accessed 27/02/2018).
Øygarden, L., Deelstra, J., Blankenberg, A.-G.B., Hauge, A., Kitterød, N.O., Eggestad, H.O., 2011. Runoff and mitigation measures in agricultural catchments under climate change in Norway. In: Kelman, I. (Ed.), Municipalities Addressing Climate Change. A Case Study of Norway. 25–49. NOVA Science Publisher, 978-1-61324-716-7, pp. 150.
Papanicolaou, A.N., Dey, S., Rinaldi, M., Mazumdar, A., 2006. Research Issues for Riverine Bank Stability in the 21st Century. IIHR Technical Report No. 457.
Pollen, N., 2007. Temporal and spatial variability in root reinforcement of streambanks: accounting for soil shear strength and moisture. Catena 69, 197–205.
Pollen, N., Simon, A., 2005. Estimating the mechanical effects of riparian vegetation on stream bank stability using a fiber bundle model. Water Resour. Res. 41 (7), 1–11.
Pollen-Bankhead, N., Simon, A., 2009. Enhanced application of root-reinforcement algorithms for bank-stability modeling. Earth Surf. Process. Landf. 34, 471–480. https://doi.org/10.1002/esp.1690.
Schaap, M.G., Leij, F.J., van Genuchten, M.Th, 2001. ROSETTA: A computer program for estimating soil hydraulic parameters with hierarchical pedotransfer functions. J. Hydrol. 251 (3-4), 163–176.
Schmidt, K.M., Roering, J.J., Stock, J.D., Dietrich, W.E., Montgomery, D.R., Schaub, T., 2001. The variability of root cohesion as an influence on shallow landslide susceptibility in the Oregon Coast Range. Can. Geotech. J. 38, 995–1024.
Sidle, R.C., 1991. A conceptual model of changes in root cohesion in response to vegetation management. J. Environ. Qual. 20, 43–52.
Sidle, R.C., Ziegler, A.D., Negishi, J.N., Nik, A.R., Siew, R., Turkelboom, F., 2006. Erosion processes in steep terrain – truths, myths, and uncertainties related to forest management in Southeast Asia. For. Ecol. Manag. 224, 199–225.
Simon, A., Collison, A.J.C., 2002. Quantifying the mechanical and hydrologic effects of riparian vegetation on streambank stability. Earth Surf. Process. Landf. 27 (5), 527–546.
Simon, A., Curini, A., Darby, S.E., Langendoen, E.J., 1999. Streambank mechanics and the role of bank and near-bank processes in incised channels. In: Darby, S.E., Simon, A. (Eds.), Incised River Channels: Processes, Forms, Engineering, and Management. John Wiley & Sons, London, pp. 123–152.
Simon, A., Curini, A., Darby, S.E., Langendoen, E.J., 2000. Bank and near-bank processes in an incised channel. Geomorphology 35, 193–217.
Skarbøvik, E., 2016. Uttesting av metoder for kvantifisering av kanterosjon i leirvassdrag, og betydning av kanterosjon for fosfortap til vannforekomstene (Bank erosion in streams - Assessment of quantification methods and importance for phosphorus losses. In Norwegian). Vann 01, 30–42.
Skarbøvik, E., Bechmann, M., 2010. Some characteristics of the Vansjø-Hobøl (Morsa) catchment. Bioforsk Rep. 128 (5), 44.
Skarbøvik, E., Haande, S., Bechmann, M., 2014. Overvaking Vansjø/Morsa 2011–2012. Resultater fra overvakingen i perioden oktober 2011 til oktober 2012 (Monitoring of Vansjø/Morsa 2011–2012. Results from monitoring period from October 2011 to October 2012). Bioforsk Rep. 71 (8), 164.
Thorne, C.R., 1990. Effects of vegetation on riverbank erosion and stability. In: Thornes, J.B. (Ed.), Vegetation and Erosion. Wiley, Chichester, pp. 125–144.
Thorne, C.R., Tovey, N.K., 1981. Stability of composite river banks. Earth Surf. Process. Landf. 6, 469–484.
Tohari, A., Nishigaki, M., Komatsu, M., 2007. Laboratory rainfall-induced slope failure with moisture content measurement. J. Geotech. Geoenviron. 133 (5), 575–587.
Vergani, C., Chiaradia, E., Bischetti, G., 2012. Variability in the tensile resistance of roots in Alpine forest tree species. Ecol. Eng. 46, 43–56.
Waldron, L., 1977. The shear resistance of root-permeated homogeneous and stratified soil. J. Soil Sci. Soc. Am. 41, 843–849.
Wu, T., Watson, A., 1998. In situ shear tests of soil blocks with roots. Can. Geotech. J. 35, 579–590.